International Journal of Pharmaceutics 417 (2011) 204–215

Contents lists available at ScienceDirect

International Journal of Pharmaceutics

journal homepage: www.elsevier.com/locate/ijpharm

Monitoring of internal pH gradients within multi-layer tablets by optical methods and EPR imaging

Friederike Eisenächer, Andreas Schädlich, Karsten Mäder*

Martin Luther University Halle-Wittenberg, Department of Pharmaceutical Technology and Biopharmaceutics, D-06120 Halle, Saale, Germany

ARTICLE INFO

Article history:
Received 7 September 2010
Received in revised form 1 October 2010
Accepted 1 October 2010
Available online 10 October 2010

Keywords:
pH dependent solubility
EPR
MRI
Benchtop NMR
Multi-layer tablet
Weakly acidic drug

ABSTRACT

The high variability of gastrointestinal pH is a general challenge regarding constant release from oral drug delivery systems, especially for ionisable drugs. These drugs often show a pH-dependent solubility and therewith associated intra- and inter-individual variability of emerging drug plasma levels. Several strategies have been investigated with the intention to influence the microenvironmental pH (pH_M) within solid formulations and therefore achieve pH-independent release profiles. Because of the heterogeneity of solid systems, a precise prediction of the occurring pH_M is rather difficult. It is therefore important to monitor the pH_M within the formulations to achieve requested release as well as to minimise pH-dependent degradation processes of the active compound. The purpose of the current study was the analysis of pH_M gradients within 2- and 3-layer tablets during hydration using 3 different techniques for comparison intensions, in particular a pH indicator dye, fluorescence imaging and EPR imaging. The influence of the presence or absence of pH modifying substances and of an additional lipophilic inter layer on the pH_M was investigated as well as the variation of matrix forming excipient and buffer pH. The influence of the pH_M on drug release was analysed as well. In addition, benchtop MRI was accomplished to gain a deeper insight on the hydration and erosion behaviour of 2- and 3-layer tablets.

1. Introduction

The oral route is still the most commonly used way for the application of drugs because of its convenient administration leading to high patient compliance. However, the variability of physiological conditions within the human gastrointestinal tract (pH, gastric residence time, intestinal motility, food intake) can be a serious challenge for a predictable release and effect of oral drug delivery systems (Grundy and Foster, 1996). Especially the variability of the gastrointestinal pH has shown to be an important parameter for drugs with ionisable functional groups (weak acids/bases). In most cases, the unionized form shows a low aqueous solubility leading to changed solubility under acidic (stomach) and neutral (intestine) conditions. The dissolution rate of a drug with diffusion-controlled release behaviour is dependent on the solubility of the drug in the diffusion layer (Gibaldi, 1984). Thus, pH-dependent solubility may lead to incomplete drug release and remarkable intra- and inter-individual variability of emerging drug plasma levels.

The concept of microenvironmental pH (pH_M) is often used in conjunction with solid formulations characterising the pH, which is generated within the formulation during hydration by surrounding media or humidity (Siepe et al., 2006; Badawy and Hussain, 2007). The pH_M has shown to affect drug stability inside solid formulations as well as dissolution behaviour, both influencing the bioavailability of an active compound (Badawy and Hussain, 2007). For this reason, several attempts have been published with the intention to modify and measure the pH_M within solid formulations to achieve pH-independent release or enhance storage stability of weakly acidic and basic drugs. One strategy is the incorporation of enteric polymers into hydrogel matrix devices. These polymers show a pH dependent solubility and are supposed to act as pore formers (Akiyama et al., 1994; Streubel et al., 2000) and pH modulators (Tatavarti et al., 2004) for weakly basic drugs. Another attempt is to influence the pH_M by incorporation of pH modifying substances. Organic acids, showing different solubilities and acid strengths, were used to enhance the release of weakly basic drugs (Thoma and Zimmer, 1990; Streubel et al., 2000; Varma et al., 2005; Siepe et al., 2006; Tatavarti and Hoag, 2006; Gutsche et al., 2008). On the other hand, basic salts were reported to improve the release of weak acids (Doherty and York, 1989; Riis et al., 2007; Tran et al., 2008).

The pH_M is influenced by many factors including excipients, active compounds, amount of water penetration, diffusion processes and pH of surrounding media. Therefore, a certain prediction is rather difficult. There is a need to monitor the local pH within solid formulations to optimise the pH_M regarding drug stability

* Corresponding author. Tel.: +49 345 55 25167; fax: +49 345 55 27029.
E-mail address: Maeder@pharmazie.uni-halle.de (K. Mäder).

0378-5173/$ – see front matter © 2010 Elsevier B.V. All rights reserved.
doi:10.1016/j.ijpharm.2010.10.010

and requested drug release. Although the pH of solutions is easy to determine potentiometrically, it is much more challenging to analyse the pH_M of solid or nearly solid formulations. Several techniques were used to gain information on the pH_M, however, there are no well-established methods available for all purposes. Diffuse reflectance spectroscopy was used to determine the pH_M of dry tablets (Glombitza et al., 1994; Glombitza and Schmidt, 1995; Scheef et al., 1998; Zinchuck et al., 2005, Pudipeddi et al., 2008). However, only the surface pH could be determined and possible interactions between the pH sensitive dye and excipients should be kept in mind. Incorporation of pH indicator dyes and following examination of occurring colours over time of hydration was also reported (Streubel et al., 2000; Varma et al., 2005; Adhikary and Vavia, 2008; Ching et al., 2008). This dye method was easy to apply but only a rough, imprecise estimation could be obtained. To achieve information concerning pH_M within the tablet core during contact with buffer, tablets had to be cross-sectioned. Another attempt was the usage of a surface pH electrode to analyse the surface pH_M of solid dispersions (Tran et al., 2008) as well as the pH_M of cryosections of hydrated tablets (Gutsche et al., 2008). Again, to gain insight on the pH_M of the inner regions, tablets had to be cut in pieces. Confocal laser scanning microscopy was used to non-invasively image pH sensitive fluorescent dyes, giving a spatial resolution of pH_M (Cope et al., 2002; Li and Schwendeman, 2005). One restriction of this technique is the limited object size, thus, only eroding microspheres were analysed. Electron paramagnetic resonance (EPR electron spin resonance, ESR) spectroscopy allows the non-invasive detection of paramagnetic compounds. The majority of drug delivery devices are not directly detectable by EPR because of the absence of naturally occurring radicals. Thus, it is necessary to incorporate paramagnetic substances e.g. stable nitroxide radicals within the objects of interest. Depending on the used substance (so called spin probe), information about microviscosity, micropolarity and pH_M inside drug delivery systems can be obtained based on the spectral sensitivity of the nitroxides to their environment (Mäder et al., 1997; Brunner et al., 1999; Lurie and Mäder, 2005; Kempe et al., 2010). EPR imaging now combines spectral information with the spatial distribution of a spin probe. Therefore, EPR imaging can be used as continuous, non-invasive technique for the spatial determination of pH_M within hydrated devices.

The purpose of the current study was the analysis of pH_M gradients within multi-layer tablets (2- and 3-layer tablets). Multi-layer tablets can be used for different purposes. It is possible to separate incompatible substances as well as to combine immediate- and prolonged-release profiles of an active compound. Furthermore, floating multi-layer tablets were developed for gastric retention consisting of a floating and a drug-containing tablet layer (Ingani et al., 1987; Wei et al., 2001; Rahman et al., 2006). The aim was to investigate the influence of (1) the presence or absence of pH modifying substances within tablet layers, (2) the variation of matrix forming excipients, (3) the variation of the pH of surrounding buffer and (4) the incorporation of an additional lipophilic inter layer on the pH_M within multi-layer tablets. The influence of the pH_M on the drug release of two model drugs, Metformin-HCl and Ketoprofen, was also analysed. An internal buffer system (IBS) composed of citric acid and disodium hydrogenphosphate was used as pH modifier. The IBS was incorporated either in one or two tablet layers to generate a pH_M gradient within the tablets. Furthermore, different matrix forming excipients were analysed for their ability to maintain a specified pH_M over time of buffer contact. Hydroxypropylmethylcellulose (HPMC) was analysed as most frequently used hydrophilic polymer which is able to form hydrogel matrices upon contact with water. HPMC is a non-ionic cellulose ether forming a stable hydrogel over the pH range of 3–11. Kollidon SR, a commercially available excipient in the form of a physical mixture of 8 parts of polyvinylacetate (PVAc) and 2 parts of polyvinylpyrrolidone (PVP), was used as well. Kollidon SR shows excellent tabletting properties and can be used for direct compression (BASF AG, 1999). Because of its aqueous solubility, PVP acts as pore former during contact with water and therefore facilitates drug diffusion. Sponge-like matrices can be observed after 12 h of buffer contact. Three different techniques were used to determine the pH_M within multi-layer tablets for comparison of results regarding application spectrum and expenses, in particular, a pH indicator dye, fluorescence imaging and EPR imaging. In addition to the analysis of the pH_M, the hydration behaviour of 2- and 3-layer tablets was monitored using nuclear magnetic resonance imaging (NMR-imaging/MRI) in order to gain a deeper insight on proceeding hydration and erosion processes during contact with buffer. MRI has proven to be a non-invasive, well established method to investigate drug delivery systems in vitro and in vivo (Richardson et al., 2005; Metz and Mäder, 2008; Nott, 2010). A commercial, low-cost benchtop MRI (BT-MRI) system was used as alternative to common superconducting MRI machines. Recently, BT-MRI has been successfully used to characterise different solid drug delivery devices (Metz et al., 2007; Strübing et al., 2008a,b; Malaterre et al., 2009). Therefore, BT-MRI was intended to provide detailed information about the differences in the hydration behaviour of 2- and 3-layer tablets.

2. Materials and methods

2.1. Materials

Kollidon® SR was kindly supplied by BASF, Ludwigshafen, Germany. Disodium hydrogenphosphate dihydrate and citric acid were obtained from Carl Roth GmbH & Co KG, Karlsruhe, Germany. They were ground in a mortar and passed through a 250 μm sieve for further use. Aerosil® was purchased from Evonik Degussa GmbH, Essen, Germany. Magnesium stearate was obtained from Magnesia GmbH, Lüneburg, Germany. Lactose-monohydrate was purchased from Euro OTC Pharma GmbH, Bönen, Germany. Methocel K100 CR was kindly supplied by Colorcon GmbH, Idstein, Germany. The fluorescence dye Carboxy SNARF®-1 was purchased from Invitrogen GmbH, Darmstadt, Germany. Bromocresol purple was obtained from Merck KGaA, Darmstadt, Germany. EPR spin probe 4-Amino-2.2.5.5-tetra-methyl-3-imidazoline-1-oxyl (AT) was obtained from N.N. Vorozhtsov Institute of Organic Chemistry, Novosibirsk, Russia. Metformin-HCl was purchased from Biotrend Chemicals AG, Wangen/Zurich, Switzerland. Ketoprofen was obtained from Sigma–Aldrich Chemie GmbH, Steinheim, Germany.

2.2. Preparation of tablets

The powder mixtures for the manufacturing of tablets were prepared according to compositions shown in Table 1 by blending all ingredients except magnesium stearate with pestle and mortar for 10 min. After adding magnesium stearate, the mixtures were blended for another 2 min. For the preparation of 2- and 3-layer tablets, weighed amounts of the different layers were fed successively into the die of the tablet press and precompacted manually. The final compression force was adjusted to receive tablets with a crushing force of 75 N after compression. Biconvex 2-layer tablets consisting of 200 mg of KSR-P or KSR layer and 100 mg of HPMC-P or HPMC layer were prepared by direct compression using a rotary tablet press (RL 12, Kilian GmbH & Co KG, Germany). Resulting 2-layer tablets had a weight of 300 mg and a diameter of 9 mm. Furthermore 3-layer tablets with an additional inter layer of 50 mg of glycerol monostearate were produced. The inter layer should achieve a better adhesiveness of both layers and decrease diffusion processes between the layers. All analysed tablet preparations are illustrated in Fig. 1.

Table 1
Composition of powder mixtures for tablet preparation (Metformin-HCl (MF) and Ketoprofen (Keto) were used as model drugs).

Components (%)	KSR layer	KSR-P layer	HPMC layer	HPMC-P layer	KSR drug layer	KSR-P drug layer
Kollidon SR	70.0	70.0	–	–	70.0	70.0
Lactose	28.5	17.4	43.5	32.4	11.1	–
Methocel K100	–	–	55.0	55.0	–	–
$Na_2HPO_4 \times 2H_2O$	–	9.9	–	9.9	–	9.9
Citric acid $\times$ H_2O	–	1.2	–	1.2	–	1.2
Drug (MF/Keto)	–	–	–	–	17.4	17.4
Aerosil	0.5	0.5	0.5	0.5	0.5	0.5
Mg-stearate	1.0	1.0	1.0	1.0	1.0	1.0

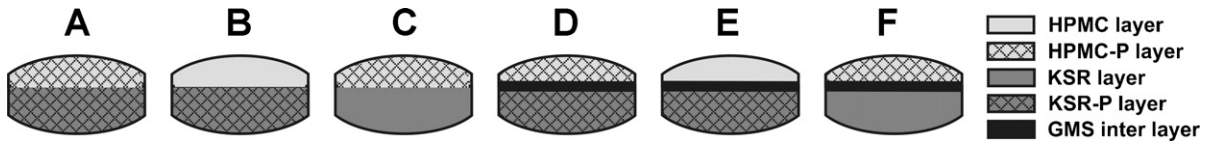

Fig. 1. Tablet compositions of tablets A–F, each tablet consisted of 200 mg KSR/-P layer and 100 mg of HPMC/-P layer, an additional inter layer of glycerol monostearate (GMS, 50 mg) was included in 3-layer tablets D–F.

2.3. Microacidity measurements using a pH indicator dye

Tablets, containing bromocresol purple (1 mg/layer) as pH indicator dye, were prepared as described before. These tablets were subjected to 100 ml of a citric acid/phosphate buffer consisting of 0.01 M citric acid solution and 0.02 M disodium hydrogenphosphate solution in a ratio of 4:1 with a resulting pH of 3 (=buffer pH 3). The pH 3 of the surrounding buffer was used as typical pH of the late phase of the fed stomach (Jantratid et al., 2008) which is important especially for gastroretentive systems. Photographs of the tablets as whole and cross-sectioned were taken after predefined time intervals (10 min, 2 h, 4 h and 6 h) of contact with buffer with a digital camera (μ850 SW, Olympus, Japan). Every tablet could be analysed only once, therefore, a new tablet incubated in the buffer for the dedicated time interval was used for every photograph. The pH of the buffer was analysed regularly and showed a stable pH of 3.

2.4. Microacidity measurements using multispectral fluorescence imaging

2-Layer tablets, containing the fluorescence dye Carboxy SNARF®-1 (0.2 μmol/g powder), were used. The tablets were placed into tubes with the diameter of the tablets and two open ends to allow a constant measuring area and a one-dimensional hydration only from top and bottom of the tablet. The tubes with incorporated tablets were transferred to 100 ml of buffer pH 3 (see Section 2.3). They were removed from the buffer at different time points and analysed by fluorescence imaging. The measurements were done with a Maestro™ in vivo imaging system (Cambridge Research & Instrumentation, Woburn, USA). A green and a yellow filter set were used. Multispectral imaging cube sets were acquired in 2 nm steps using automatic exposure times. Averaged spectra were extracted from different image regions to allow a pH_M calculation of both tablet layers. The ratios of the maxima were determined. Corresponding pH_M values were calculated using a calibration curve of the fluorescence dye. Furthermore, pseudo-coloured fluorescence images were generated by separating the microacidities of the measured images using an acidic spectrum (assigned colour red) and a neutral spectrum (assigned colour green) of the spectra library. The measured spectrum of each data point was assigned to the closest matching spectrum. Therefore, acidic domains of the measured tablets appear red; areas with a pH > 6 appear green within the pseudo-coloured images.

2.5. Microacidity measurements using spatial spectral EPR imaging

2- and 3-layer tablets containing EPR spin probe AT (1 μmol/g powder) were used. Measurements were performed with a L-band EPR spectrometer (Magnettech GmbH, Berlin, Germany) using following parameters: B_0-field 48.9 mT, scan range 8 mT, scan time per projection 30 s, modulation amplitude 0.1 mT, attenuation 6 dB, maximum gradient of 2.5 mT/cm, points per projections 1024, 31 projections/6 missing projections, image reconstruction giving an image matrix of 512 × 512 points and a spatial resolution of about 200 μm. The KSR/KSR-P layer of the tablet used for analysis was glued to a plastic bar which was placed into 100 ml of buffer pH 3 (see Section 2.3). The plastic bar with the affixed tablet was removed from the buffer at different time points. Adhering water on the surface of the tablet was removed carefully using absorbent paper before measuring. Two dimensional EPR images were collected for all tablet compositions after 10 min, 30 min, 1, 2, 3, 4 and 6 h of buffer contact. The pH of the buffer was analysed regularly and showed a stable pH of 3. The EPR spectra of the different image layers were extracted from the images. Only image domains with signal intensities over 30% were used for further analysis. The values of $2a_N$ (distance 1st to 3rd peak) were determined from the extracted spectra. Resulting pH_M values were obtained using a pH calibration curve of AT and plotted against the spatial position within the tablet. Experiments were performed in triplicate.

2.6. Influence of the microenvironmental pH on the drug release

Dissolution studies were carried out to investigate if different pH_M within a tablet could influence the drug release. Metformin-HCl and Ketoprofen were used as model drugs. Drug containing tablets were prepared by incorporating 17.4% of drug instead of lactose into the Kollidon SR layer giving a drug content of 34.8 mg per tablet (Table 1). The drug release was determined from 2-layer tablets B and C and 3-layer tablets E and F. Dissolution studies were carried out with an automatic dissolution tester (PTWS 310, Pharmatest Apparatebau, Hainburg, Germany) in 900 ml of buffer pH 3 (see Section 2.3) at 37 °C and 50 rpm. The drug release was analysed by measuring UV absorbance at 233 nm for Metformin-HCl, and 275 nm for Ketoprofen and calculated using calibration curves. Dissolution experiments were carried out over 12 h and performed in triplicate.

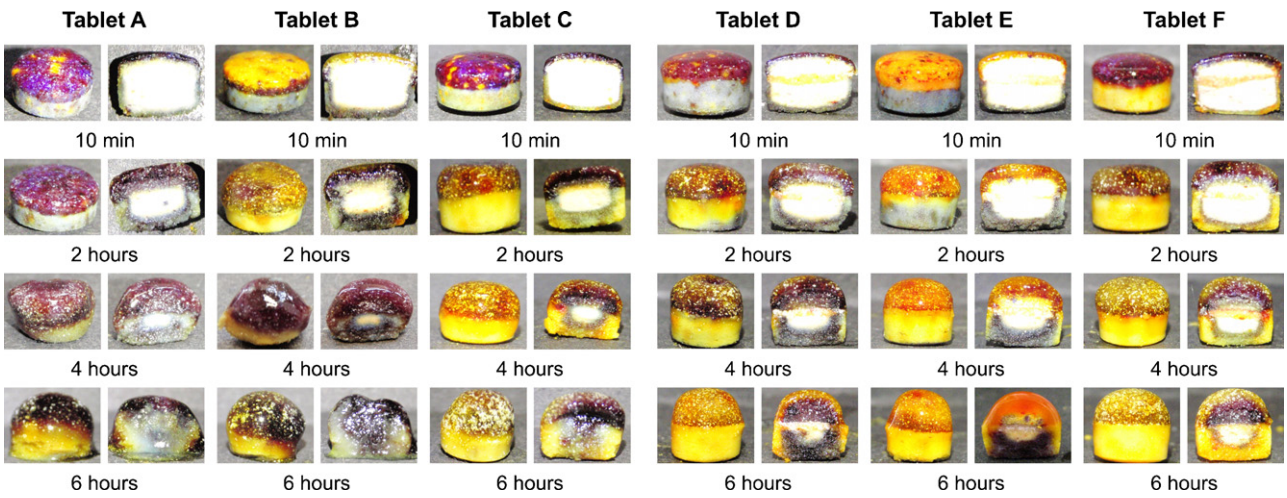

Fig. 2. Images and cross-sectional images of hydrated matrices of tablets A–F after different time intervals of contact with buffer pH 3. Tablets were always placed with the HPMC layer on top and the KSR layer as bottom side. Purple (dark grey or black) domains indicate a pH > 5, yellow (light grey) domains indicate a pH < 4.5. The dry core appeared white. (For interpretation of the references to colour in this figure legend, the reader is referred to the web version of the article.)

2.7. Monitoring of hydration behaviour by means of NMR benchtop imaging

NMR imaging experiments were performed on a BT-MRI spectrometer working at a frequency of 20 MHz and using a static magnetic field (B_0) of 0.5 T (Maran DRX2, Oxford Instruments Molecular Biotools, Oxfordshire, UK). A standard spin-echo sequence was used with an echo time of 9.8 ms and a repetition time of 300 ms leading to an acquisition time of about 5 min for each image. Sixteen scans were accumulated to obtain 64 × 64 pixel images with a field of view of 4 cm^2, which led to an in-plane resolution of 312.5 μm. 2- and 3-layer tablets were placed in a USP paddle dissolution apparatus with 900 ml of buffer pH 3 of 37 °C, stirred at 50 rpm, or in a beaker with 100 ml of same buffer at room temperature without stirring. The tablets were removed for MRI measurements after predefined time intervals and transferred to a sample holder. T_1-weighted MRI images were measured after 10 min, 30 min, 1, 2, 3, 4 and 6 h of contact with buffer. Experiments were performed in triplicate. MRI intensity profiles of resulting images were investigated using Oxford Instruments RIImageJ VO.NIX as plug-in for Image J.

3. Results

3.1. Microacidity measurements using a pH indicator dye

The microenvironmental pH of hydrating multi-layer tablets was visualised using the pH indicator bromocresol purple with a transition pH range of 5.2–6.8 and a colour change from yellow to purple. This dye was used to differentiate between tablet layers which assumed the pH of the surrounding buffer and areas with incorporated IBS (Na_2HPO_4/citric acid). The tablet layers with incorporated IBS were supposed to generate a pH_M of around 6 upon hydration while the pH of the surrounding buffer was 3 which enabled the monitoring of different colours depending on presence or absence of IBS. In addition, the colour change from yellow to purple could be easily monitored. Photographs of tablets A–F as whole and cross-sectioned after defined time intervals of contact with buffer are shown in Fig. 2. After 10 min of buffer contact, a differentiation between formulations A, B and C and D, E and F is easily possible. The HPMC-P and KSR-P layer of tablets A and D turned purple/blue immediately after contact with buffer, indicating a pH above 5. This finding corresponded to the expectation because the IBS was incorporated into both layers. The pH_M of the exterior region of the KSR-P layer changed to yellow after 2 h whereas the HPMC-P layer appeared mainly purple over more than 4 h. The HPMC layer of tablets B and E (without IBS) turned yellow after contact with buffer. In the case of tablet B, the HPMC layer changed into purple, indicating a pH_M above 5, after 30–60 min of buffer contact. In contrast, the HPMC layer of tablet E maintained a yellow/orange colour over the analysed time interval of 6 h. The KSR layer of tablets C and F (without IBS) turned yellow after contact with buffer. No obvious change in colour could be observed over the analysed time.

3.2. Microacidity measurements using multispectral fluorescence imaging

Multispectral fluorescence imaging of 2-layer tablets was accomplished to analyse the pH_M of the tablet surface by means of a hydrophilic fluorescence dye. The emission spectrum of this dye undergoes a pH-dependent wave length shift (Fig. 3(a)). pH_M values could be calculated independently from the intensities for a pH range from pH 5 to 8 using a calibration curve (Fig. 3(b); Schädlich et al., 2009). Pseudo-coloured fluorescence images and corresponding pH_M values of both tablet layers of tablets A, B and C are illustrated in Fig. 4. The pH_M of both layers of tablet A showed values between pH 6.5 and 7.5 over more than 6 h. Higher pH_M values were detected within the HPMC-P layer compared to the KSR-P layer. The pH_M of the HPMC layer of tablet B increased from a predominantly acidic environment below the dye detection limit of pH 5 to values above pH 6 after about 3 h of contact with buffer (Fig. 4(B)). The pH_M shifting was delayed in comparison with the pH indicator results. This observation can be explained by the hindered hydration of the tablets from only two dimensions (see Section 2.4). The pH_M of the KSR layer of tablet C remained below pH 5 over more than 6 h (Fig. 4(C)).

3.3. Microacidity measurements using spatial spectral EPR imaging

EPR imaging provides the possibility to obtain spatial information about the pH_M within the tablets non-invasively. For the investigation of the pH_M by EPR imaging, the stable nitroxide radical 4-Amino-2.2.5.5-tetra-methyl-3-imidazoline-1-oxyl (AT) was used as pH-sensitive spin probe. Protonation of pH-sensitive spin probes leads to changes in the spin density of the nitroxide group (Fig. 5(b)) and therewith associated changes in the EPR spectra

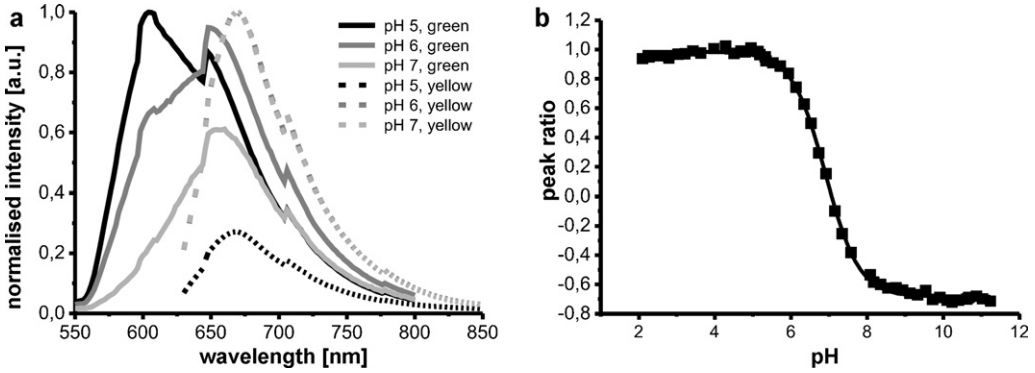

Fig. 3. (a) pH-dependent wave length shift of the emission spectrum of the fluorescence dye Carboxy SNARF®-1. A green and a yellow filter set were used. (b) pH sensitivity of the peak ratio of Carboxy SNARF®-1.

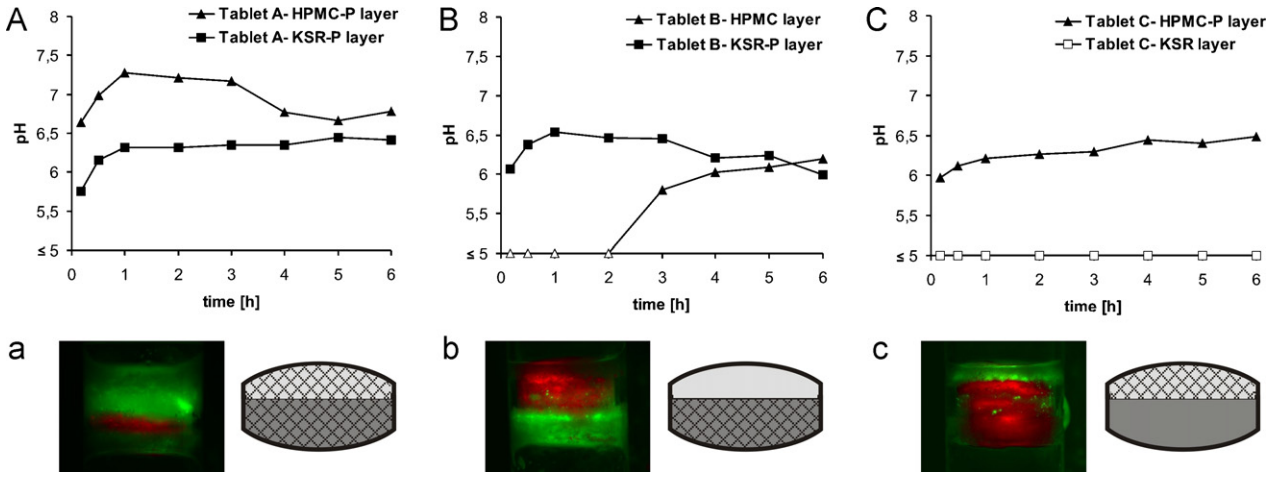

Fig. 4. (A–C) Mean pH_M values of the surface of both layers of tablets A, B and C from one dimension at different time intervals of contact with buffer pH 3. No values could be determined for areas with a pH < 5 (empty symbols). (a–c) Pseudo-coloured fluorescence images and corresponding schemata of tablets A, B and C after 30 min of buffer contact, red (dark grey) domains symbolise dry and acidic regions (pH < 5), green (light grey) domains symbolise a nearly neutral pH_M (pH > 6). (For interpretation of the references to colour in this figure legend, the reader is referred to the web version of the article.).

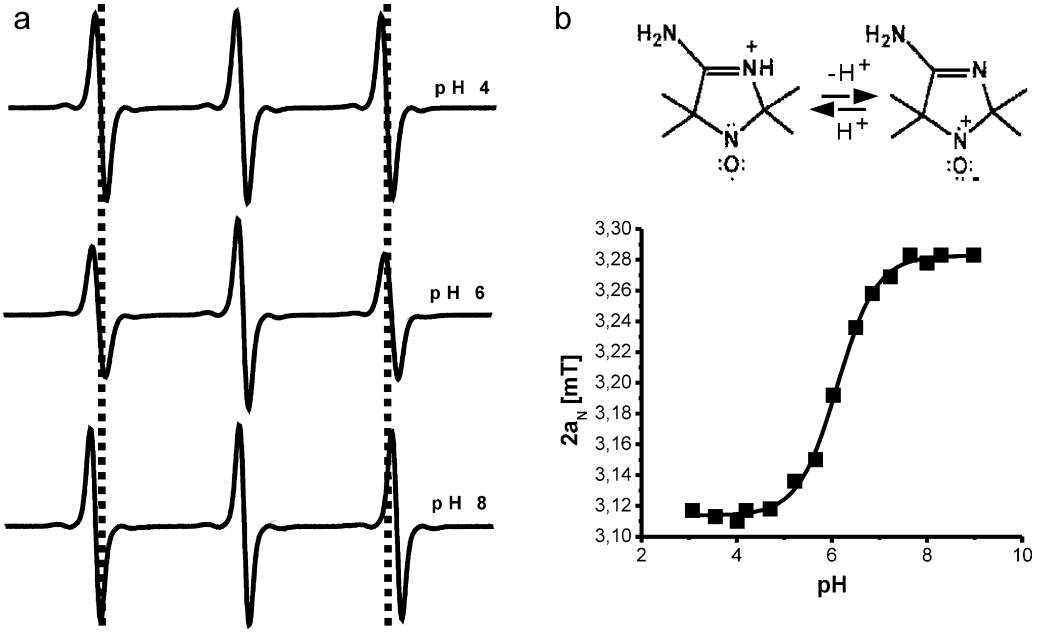

Fig. 5. (a) EPR spectra (first derivates) of the spin probe 4-Amino-2.2.5.5-tetra-methyl-3-imidazoline-1-oxyl (AT) at different pH values. The dashed line symbolises $2a_N$ (a_N = the hyperfine splitting constant) for the spectrum at pH 4. Note that the distance between the first and the third amplitude is larger for the nonprotonated form (pH 8). (b) Principle of pH sensitivity and calibration curve of AT.

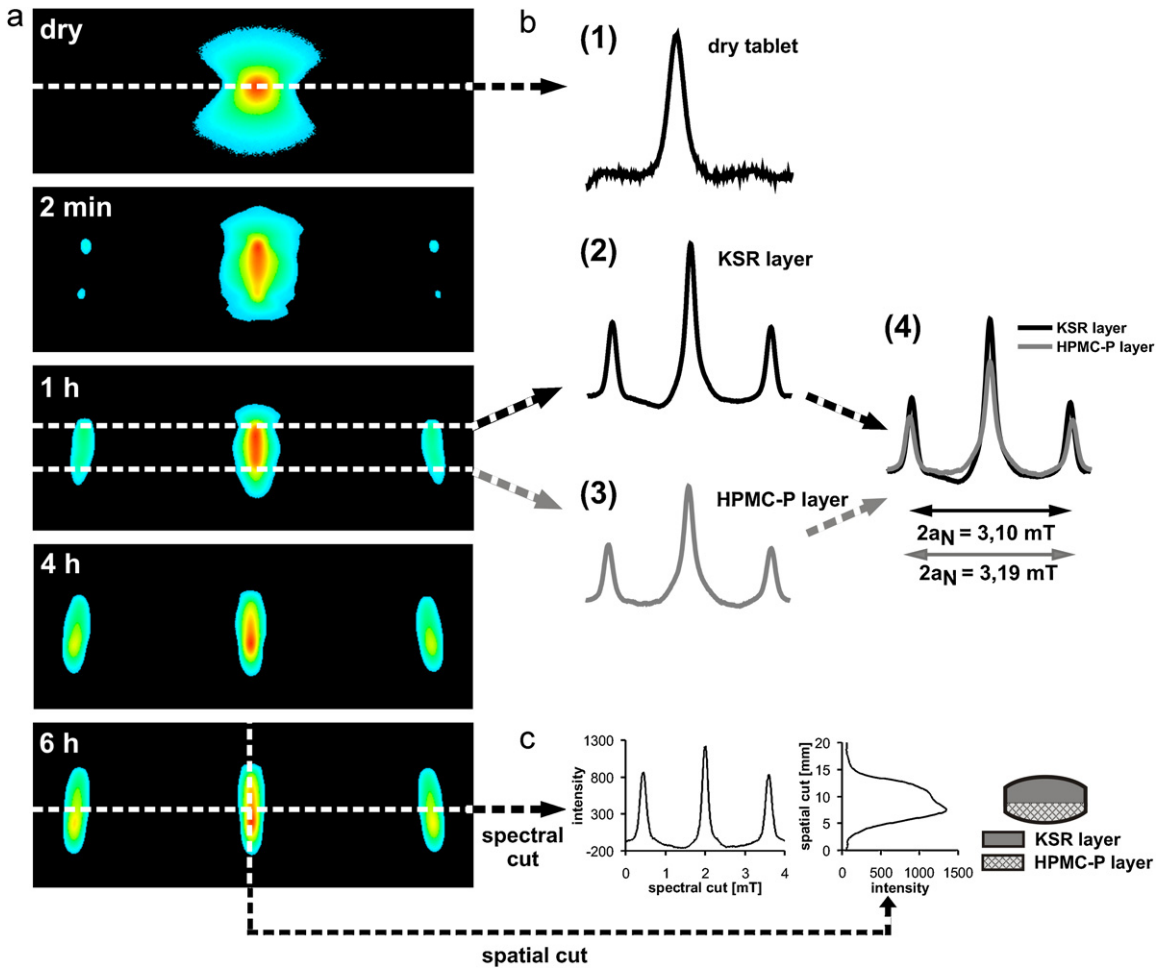

Fig. 6. (a) EPR images of AT-containing tablet C at different time intervals of contact with buffer pH 3. (b) EPR spectra which were extracted from the images of: (1) the dry tablet, (2) a region within KSR-layer after 1 h of buffer contact, (3) a region within HPMC-P-layer of the same image, (4) relation of spectra (2) and (3) with specified $2a_N$. (c) Spatial and spectral cut of tablet C after 6 h of buffer contact.

depending on pH (Fig. 5(a); Khramtsov et al., 1982). In particular, the distance of the first to the third peak ($2a_N$, where a_N is the isotropic hyperfine splitting constant) changes with changing pH of the surrounding buffer. Thus, a quantification of pH is possible by means of a calibration curve of $2a_N$ against buffer pH (Kempe et al., 2010). The pH dependency of the EPR signal of the spin probe AT follows a sigmoid dependence (Fig. 5(b)). Therefore, the pH_M calculation is only possible in a limited pH range of about ±1.5 pH units depending of the pK_a of the spin probe (pK_a of AT is 6.1). Other spin probes having different pK_a values can be used to analyse different pH ranges.

Fig. 6(a) shows characteristic EPR images of tablet C at different time points of contact with buffer. The horizontal scale symbolises the spectral resolution (3 peaks of mobile AT) while the upright scale characterises the spatial resolution from the top to the bottom of the tablet (Fig. 6(c)). The dry tablet shows only one central peak of the immobile spin probe. Contact with buffer led to an increase in mobility of AT in the hydrated regions, visible through the appearance of the outer isotropic hyperfine splitting (Lurie and Mäder, 2005). The proportion of mobile to immobile spin probe increased steadily with time, detecting the liquid penetration to inner tablet regions which can be observed by the increase of intensity of the isotropic hyperfine splitting. It was also possible to follow the swelling process of the tablets because of the increase in spatial signal size of the images over time. The signals indicate a pH gradient within the wet tablet which is visible by the changing distance from first to third peak (both sloped outwards). EPR spectra were extracted out of the horizontal layers of the presented images. Fig. 6(b) shows typical EPR spectra of: (1) a dry tablet; (2) the KSR layer after 1 h of buffer contact and (3) the HPMC-P layer of the same EPR image. By comparison of spectra (2) and (3), a changing distance of $2a_N$ can be found (4). $2a_N$ of spectrum 2 (KSR layer) underlay the calculable range, indicating a pH_M below 4.5. The calculated pH value of spectrum 3 (HPMC layer) was 6.03 which can be explained by the presence of IBS within this layer.

Spatial resolved pH_M values extracted from the EPR images of tablets A, B and C at different time intervals of buffer contact are presented in Fig. 7. The pH_M of whole tablet A was found to be around pH 6 for over 6 h (Fig. 7(A)). The acidic pH_M of the HPMC layer of tablet B increased quite fast to more neutral values above pH 6 (Fig. 7(B)) while the predominantly acidic pH_M of the KSR layer of tablet C changed only marginally in the centre region of the tablet (Fig. 7(C)). EPR imaging experiments of tablets A–F were repeated using a citric acid/phosphate buffer of pH 5.5 to gain information of the influence of the pH of the surrounding buffer on the pH_M. Similar results concerning the formation of pH_M gradients within tablets over time of buffer contact were obtained. Fig. 7(C2) shows the pH_M gradients within tablet C during contact with buffer pH 5.5. Interestingly, the pH_M of the KSR layer was below the pH of the surrounding buffer up to 1 h of buffer contact. A 10% Kollidon SR suspension in water generates a pH of about 4.6. Thus, Kollidon SR could cause the more acidic pH_M. After 1 h, the KSR layer assumed the pH of the surrounding buffer. The pH_M increased to values above

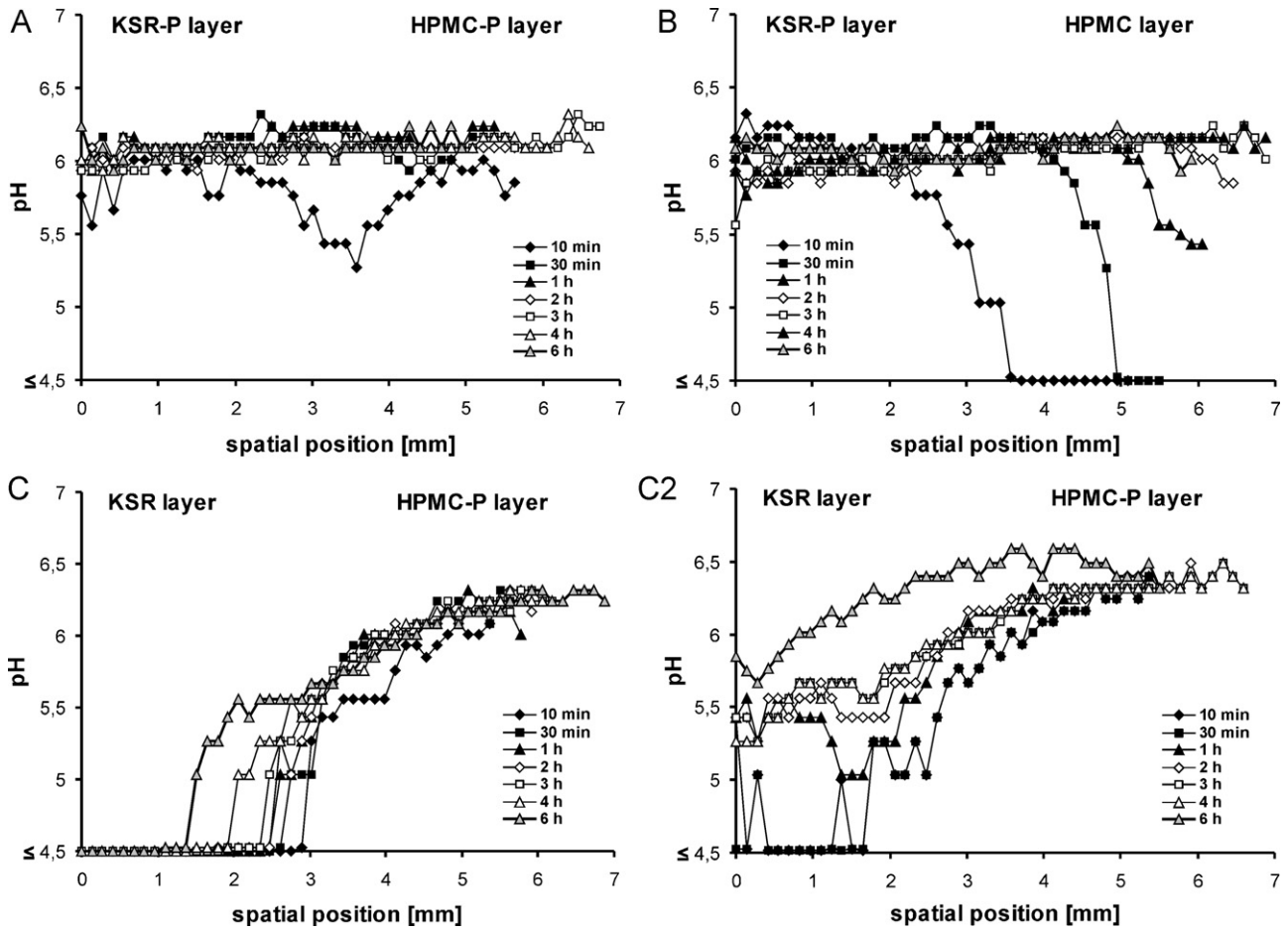

Fig. 7. (A–C2) pH_M averages within tablets A, B and C calculated from EPR images which were generated at different time intervals of contact with buffer pH 3. A buffer of pH 5.5 was used in the case of (C2). No values could be determined for areas with a $pH_M \leq 4.5$.

pH 6 after 6 h of buffer contact, possibly caused by the penetration of HPMC-P gel of low viscosity.

3-Layer tablets with an additional inter layer were analysed subsequently. The inter layer was added to enhance the integrity of both layers as well as to decrease diffusion processes between the layers. Fig. 8 demonstrates the differences in the EPR images of a 2- and a 3-layer tablet. The image of the 2-layer tablet C shows one homogeneous central signal. The central signal of the image of the 3-layer tablet F shows two separate areas of high intensity (red colour/dark grey). This difference is also obvious in the intensity profiles I in Fig. 8(b). The signal interruption of I_2 was caused by the lipophilic inter layer without spin probe. The transition of HPMC-P to KSR layer could be considerably monitored within the outer signals of image F because of a visible change of the distance of the first to the third peak ($2a_N$). Intensity profiles II and III illustrate a gradient within the right signal which is sloped outwards, thus indicating a pH_M gradient within the tablets.

pH_M profiles of tablets D–F over 6 h of buffer contact are presented in Fig. 9(D–F). Tablet D shows similar results like tablet A. The pH_M of the HPMC-P and the KSR-P layer lay around pH 6 over the analysed time interval. The HPMC layer of tablet E maintained an acidic pH_M over 6 h, which was different compared to tablet B. The inter layer seemed to hinder the approximation of pH_M of both layers. The protective character of the inter layer became also apparent in the case of tablet F. A sharp increase of the pH_M separates the acidic values of the KSR layer from the nearly neutral values of the HPMC-P layer over more than 6 h of buffer contact. The slight displacement over time may be caused by the swelling of the KSR layer.

3.4. Influence of the microenvironmental pH on the drug release

Dissolution studies of two model drugs were carried out to investigate the influence of the pH_M on the drug release. The antidiabetic drug Metformin-HCl was used as freely soluble model drug showing pH independent release behaviour. Primarily, the drug release from 2-layer tablets was analysed. Unfortunately, these tablets could not withstand the release conditions and both tablet layers separated after about 2 h of dissolution testing. The layer separation led to an increase in dissolution rate of Metformin-HCl caused by the increased diffusion area (Fig. 10(a)). An additional inter layer of glycerol monostearate could considerably enhance the integrity of the tablets and prevent the separation of both tablet layers over the analysed time interval. Fig. 10(b) demonstrates the release behaviour of Metformin-HCl from 3-layer tablet formulations E and F. The IBS was present in the KSR-P layer of tablet E; while none was present in the KSR layer of tablet F. As expected, no influence of the pH_M on the drug release of Metformin-HCl could be found.

In contrast, NSAID Ketoprofen was analysed as model drug showing a pH dependent solubility. Ketoprofen is very slightly soluble at acidic pH (0.28 mg/ml at pH 4) and slightly soluble at pH 6.0 (3.68 mg/ml) (Sheng et al., 2006). The solubility increases with increasing pH because of the cumulative deprotonation of the carboxyl group (pK_a of 4.76). Fig. 10(c) demonstrates the dissolution profiles of Ketoprofen from 3-layer tablets E and F. Tablet formulation E enhanced the drug release considerably in comparison to tablet formulation F. The drug containing KSR-P layer of tablet E generated a pH_M of around 6, thus, leading to a higher solubility of

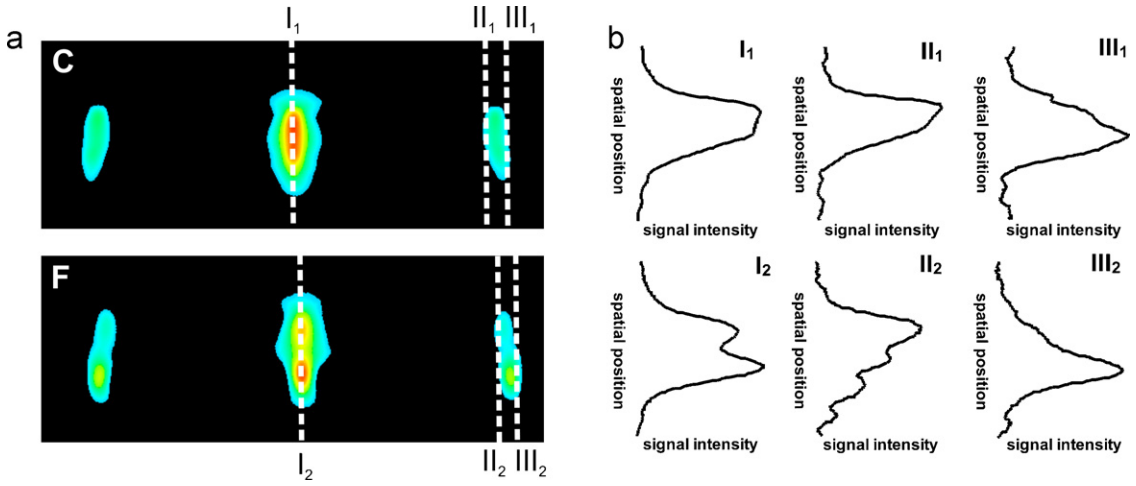

Fig. 8. (a) EPR images of tablets after 1 h of contact with buffer pH 3, the dotted lines show the position of the intensity profiles displayed in (b). Image C: 2-layer tablet C. Image F: 3-layer tablet F. (b) intensity profiles of the EPR signal of: (I) the central peak; (II) the left region of the right peak; (III) the right region of the right peak.

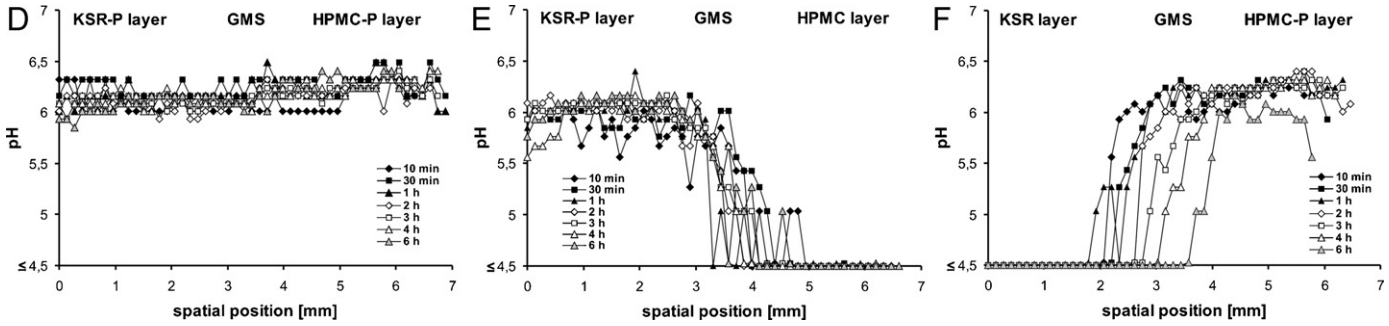

Fig. 9. (D–F) pH_M averages within tablets D, E and F calculated from EPR images which were generated at different time intervals of contact with buffer pH 3. No values could be determined for areas with a $pH_M \leq 4.5$.

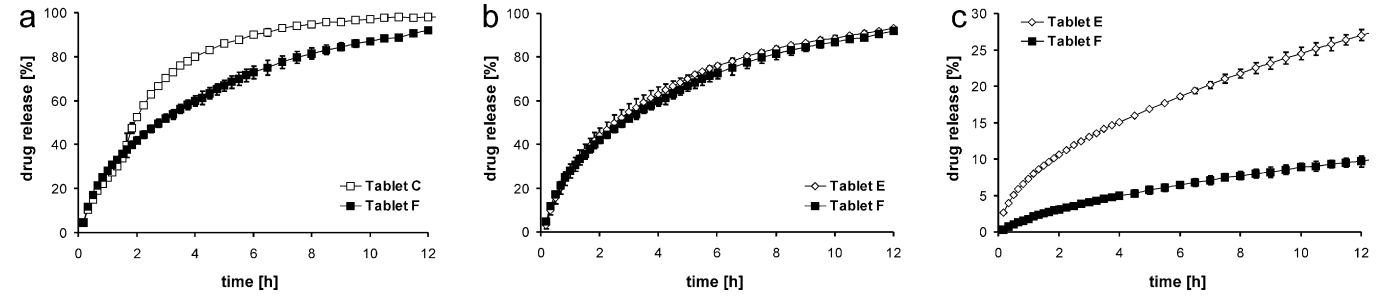

Fig. 10. Drug release in buffer pH 3. (a) Metformin-HCl release from 2-layer tablet C and 3-layer tablet F. (b) Metformin-HCl release from 3-layer tablets E and F. (c) Ketoprofen release from 3-layer tablets E and F.

Ketoprofen and therefore to an increase in drug release. The formulations were not further optimised regarding drug release, although even a drug release of around 30% over 12 h is quite low. However, the purpose of this investigation was not to develop an optimised formulation but to show the influence and importance of the pH_M within tablets on the drug release, especially for ionisable drugs.

3.5. Monitoring of hydration behaviour by means of ^{1}H NMR benchtop imaging

Fig. 11 demonstrates the schematic process of tablet hydration of both tablet constitutions which could be monitored using benchtop MRI equipment over time of buffer contact. No considerable differences could be found between tablet formulations A, B and C (data not shown). Therefore, only 2-layer tablets C and 3-layer tablets F were further investigated. The hydration of 2-layer tablets

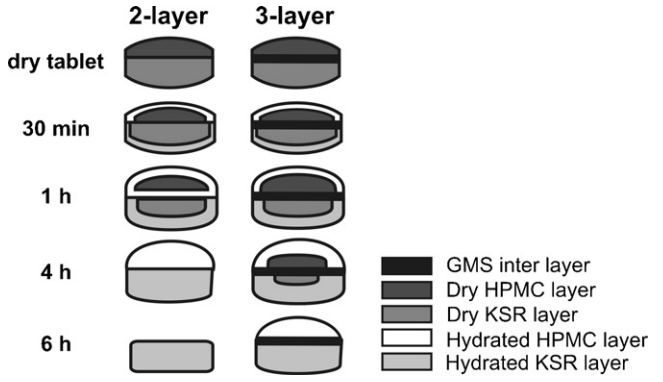

Fig. 11. Schematic process of tablet hydration of a 2- and a 3-layer tablet at different time intervals of contact with buffer.

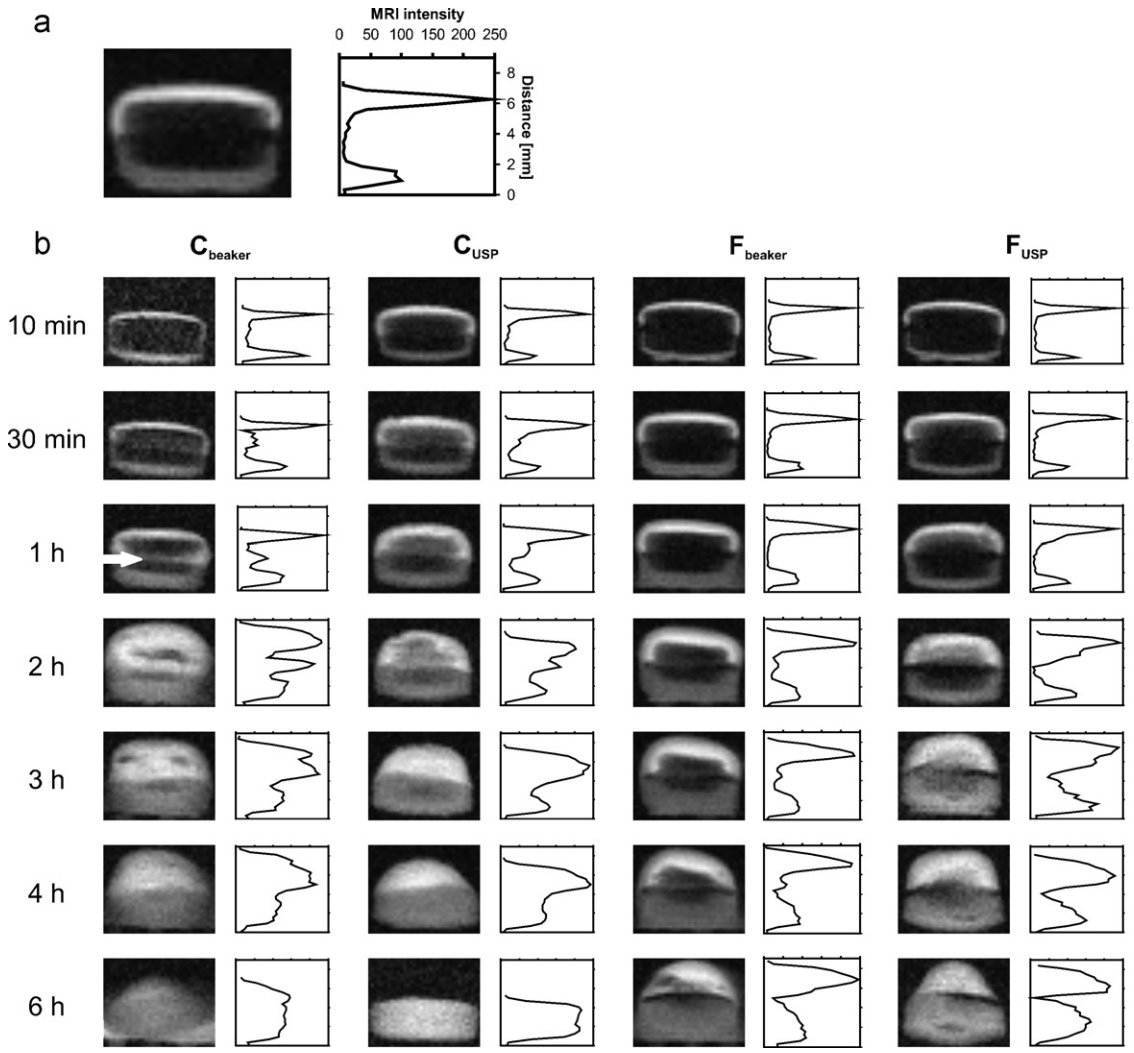

Fig. 12. (a) ^{1}H NMR benchtop magnetic resonance image and corresponding signal intensity profile of tablet preparation F after 30 min of contact with buffer, exemplified for scale labelling of (b). (b) ^{1}H NMR benchtop magnetic resonance images and corresponding signal intensity profiles of tablet preparations at different time intervals of contact with buffer. C_{beaker}: 2-layer tablet C, hydration in unstirred beaker. C_{USP}: 2-layer tablet C, hydration in USP paddle dissolution apparatus at 50 rpm. F_{beaker}: 3-layer tablet F, hydration in unstirred beaker. F_{USP}: 3-layer tablet F, hydration in USP paddle dissolution apparatus at 50 rpm. The arrow indicates the visible water penetration between both layers of tablet C.

started at the edges of the tablets but continued between the two layers, leading to a separation over time of hydration. Furthermore, diffusion processes between the layers could be facilitated. The swelling of the hydrated regions led to an increase in size. The tablets were completely hydrated after about 4 h of buffer contact. After 6 h, both layers were often separated. The additional inter layer of the 3-layer tablets prevented the penetration of water between the Kollidon SR and the HPMC layer. Therefore, the hydration process was slower because it continued only from the edges of the tablets to the inner regions. A dry core was existent even after 4 h of buffer contact. The 3-layer tablets remained complete over more than 6 h of hydration.

Characteristic T_1-weigthed BT-MRI images with corresponding intensity profiles of 2- and 3-layer tablets over time of buffer contact are presented in Fig. 12. Dark areas within the tablets refer to low spin densities and/or short relaxation times, which are related to dry parts of the tablets. Hydrated areas appear bright because of the water penetration and therewith associated increase in spin density. Relaxations times in the range of 10 up to hundred milliseconds give the brightest contrast under our measurement conditions (T_1 weighted). The HPMC layer appears brighter than the Kollidon SR layer. HPMC forms a gel upon hydration. The water inside the gel layer was not as flexible as in the pores of the Kollidon SR matrix leading to shorter T_1 relaxation times and a brighter signal which could also be confirmed by NMR relaxometry (data not shown). A swelling of the HPMC and Kollidon SR layer could be monitored by increase in size of the tablets. The different tablet formulations were exposed to two different hydration settings. Tablets exposed to USP dissolution conditions showed a faster water penetration into and erosion of the HPMC layer compared to the unstirred tablets, visible by a faster decrease in size. Water penetration between both layers of the 2-layer tablet C could be monitored after 30 min of buffer contact independent from used hydration setting which is also illustrated in the corresponding MRI intensity profiles. After 1 h, an additional central peak could be monitored within the intensity profiles (Fig. 12(b); C, 1 h). In contrast, the hydration of 3-layer tablets F proceeded only from the edges of the tablets caused by the aforementioned interference of the inter layer. The inter layer is clearly visible as black region between the HPMC and the KSR layer over the analysed time interval of 6 h. Because of its lipophilic character, almost no water penetrated into this region leading to low spin density and a black colour. The MRI intensity profiles illustrate the low signal intensity between the HPMC and the KSR layer even after 6 h of contact with buffer (Fig. 12(b); F, 6 h).

4. Discussion

The purpose of present study was the detection of pH_M gradients within multi-layer tablets. Different techniques were investigated for comparison purposes, all leading to similar results. A pH indicator dye was incorporated into tablets A–F, which allowed the differentiation between the tablet formulations because of their differences in local pH and therewith associated colour changes. Furthermore, it was possible to monitor the shifting of pH_M within the tablet layers over time of buffer contact and to observe differences in the pH_M shifting of 2- and 3-layer tablets. Nevertheless, this technique allowed only a very rough determination of the pH_M. It was rather difficult to relate a specified pH value to the colour grading of the indicator. Colours indicating same pH appeared different in both matrix forming excipients (HPMC and KSR). In addition, to investigate the pH_M in the interior of the tablet, the tablet had to be cut. It was therefore not possible to analyse the pH_M of one tablet continuously.

Fluorescence imaging gave the opportunity to calculate an average pH_M of an estimated domain of each tablet layer using a fluorescence dye with pH dependent changes in the emission spectra. Similar pH gradients were detected compared to the results of the aforementioned method. However, a different hydration setting had to be used to allow a constant measuring area which changed and delayed the hydration process and made comparison with other results rather difficult. Higher pH_M values were detected within the HPMC-P layer compared to the KSR-P layer of tablet A (same amount of IBS in both layers). The usage of different excipients could have an impact on the emission spectrum. The influence of the nature of excipient on the pH_M calculation was therefore analysed by fluorescence imaging. Kollidon SR and HPMC showed no clear trend to enhance or decrease calculated pH_M values (data not shown). A 10% Kollidon SR suspension in water generates a pH around 4.6 which also influences the resulting pH_M. Furthermore, the photographs of pH-indicator containing tablets showed a yellow discolouration of the surface of the previously blue KSR-P layer after 1–2 h (Fig. 2). In contrast, the colour of the HPMC-P layer changed only marginally. With fluorescence imaging, it was only possible to analyse the pH_M of the surface of the tablets because of the limited penetration depth of the excitation and emission light. The pH_M of the surface of the tablet could differ from those of the inner regions which can also contribute to the monitored differences.

Therefore, EPR imaging was accomplished to determine the spatial pH_M distribution of the tablets non-invasively. EPR imaging provides the possibility to calculate the average pH_M of hydrated inner and outer regions of different cylindrical layers of the tablet giving a spatial pH_M resolution from top to the bottom of the tablet. Although the analysis with this technique is more time consuming, it gave unique information about the internal pH within analysed tablets and made a continuous measurement of one tablet over time of hydration possible. Furthermore, no influence of the nature of surrounding matrix material on the resulting $2a_N$ values could be detected (data not shown). However, the pH_M calculation is only possible in a limited pH interval of about ± 1.5 pH units depending of the pK_a of the spin probe (pK_a of AT is 6.1). Therefore, no pH_M values could be calculated in tablet regions showing a pH_M below 4.5. It is possible to investigate the pH_M within more acidic regions of the tablets using a spin probe with a lower pK_a.

The pH of the buffer strongly influenced the internal pH of tablet layers without IBS. Almost no influence could be monitored in the case of tablet layers with IBS (Fig. 7(C2)). The HPMC layer of tablet B (without IBS) showed an acidic pH_M after contact with buffer but started to change to nearly neutral values after 30 min. After 2 h, the complete HPMC layer showed a pH around 6 (Fig. 7(B)). A possible reason could be the migration of IBS out of the KSR-P layer into the HPMC layer. In contrast, the HPMC layer of tablet E remained acidic over 6 h of buffer contact (Fig. 9(E)). The migration of IBS seems to be hindered by the lipophilic inter layer. In the case of the KSR layer of 2- and 3-layer tablet C and F (without IBS), an obvious pH_M gradient over more than 6 h of buffer contact was determined. Especially in the case of tablet F, the pH_M of the KSR layer showed an acidic $pH \leq 4.5$ over the analysed time interval of 6 h, confirming the protective character of the inter layer (Fig. 9(F)). This finding could also be valuable to separate drugs with different pH stability optima by the usage of multi-layer tablets with an additional lipophilic inter layer. However, the pH_M of the KSR layer of tablet C increased only marginally in the centre region of the tablet as well, which was different from the behaviour of the HPMC layer of tablet B. The different behaviour of both matrix-forming excipients might possibly be caused by a faster water exchange within the KSR layer in comparison to the HPMC layer. Furthermore, the acidic behaviour of Kollidon SR seems to have an influence on the pH_M generation as well.

Dissolution studies were carried out to analyse the influence of the pH_M on the drug release. Two model drugs were incorporated into the KSR/KSR-P layer of tablet E/F (with and without IBS). Metformin-HCl shows a pH independent solubility. Therefore, both formulations showed same drug release (Fig. 10(b)). In contrast, the release of Ketoprofen could be modified by the incorporation of the IBS. Ketoprofen shows a pH dependent solubility with an improved solubility under neutral conditions (see Section 3.4). Therefore, the drug release of tablet formulation E (with IBS) was faster compared to formulation F (without IBS) (Fig. 10(c)). These finding is in agreement with literature data where the drug release of weak acids could be improved by the incorporation of alkaline excipients (Doherty and York, 1989; Riis et al., 2007; Tran et al., 2008). Further formulation optimisation would be needed for a reasonable drug release over 12 h. This issue was beyond the scope of this work as it was intended to keep the formulation of the layers constant for comparability purposes.

Benchtop NMR imaging was accomplished to further analyse the differences in the hydration behaviour of 2- and 3-layer tablets. The MRI signal of the HPMC layer appeared brighter compared to the signal of the KSR layer. The water inside the gel layer of HPMC is not as flexible as in the pores of the KSR matrix leading to a shorter T_1 relaxation time and a brighter signal. This issue could also have an influence on the different behaviour regarding the migration of IBS. Besides, it could be detected that water penetrated between the two layers of the 2-layer tablets (Fig. 12(C)) which could enable a fast migration of IBS from the KSR-P to the HPMC layer of tablet B. Furthermore, a separation of both layers could be facilitated. The water penetration could be prevented by an additional lipophilic inter layer which improved the integrity of the tablets and possibly hindered the migration process of the IBS (Fig. 12(F)). In addition, 2- and 3-layer tablets were exposed to two different hydration settings. Tablets exposed to USP dissolution conditions showed a faster water penetration into and erosion of the HPMC layer compared to the unstirred tablets (Fig. 12). These findings are consistent with previous work, showing the dependence of erosion and hydration processes of hydrogel-forming HPMC on mechanical stress (Costa and Lobo, 2001; Kavanagh and Corrigan, 2004). Further studies have to be carried out to investigate, if mechanical stress could also change the migration behaviour of the IBS.

In conclusion, pH_M gradients within multi-layer tablets could be analysed by 3 different techniques, in particular, a pH indicator dye, fluorescence imaging and EPR imaging. It was possible to gain information about the pH_M with all applied techniques. The qualitative results were similar but the informative value showed major differences. The incorporation of a pH indicator dye turned out to be a simple, fast and inexpensive method to get an overview over proceeding processes. However, no precise pH_M determina-

tion was possible and the inner tablet regions could be analysed only invasively. Fluorescence imaging produced calculable results of the pH_M of the tablet surface. A spatial distribution of the surface pH_M could be provided. However, a different hydration setting had to be used, excipient interactions were hard to predict and the inner regions of the tablet can be analysed only by cutting the tablet. EPR imaging proved to be a powerful tool for the determination of spatial pH_M information non-invasively. However, it should be emphasised that the resulting pH_M describe an average pH_M value of a thin tablet layer, possibly forming a pH_M gradient inside this layer with different pH_M values in the outer regions compared to the centre of the tablet. Furthermore, it is a time consuming method which requires expensive equipment. Nevertheless, because of its superior advantages, EPR imaging was used as method of choice for further analysis. The influence of different variables on the pH_M was investigated. The incorporation of an IBS strongly influenced the pH_M as well as the nature of used matrix forming excipient. Kollidon SR generated a more acidic microenvironment compared to HPMC, which was obvious in particular when buffer pH 5.5 was used where the pH_M of the KSR layer underlay the buffer pH. The pH_M of the KSR layer maintained acidic over the analysed time interval. Otherwise, the HPMC layer was able to turn primary acidic pH_M to more neutral values although the acidic properties of the surrounding buffer which may be caused by the migration of IBS from the KSR-P layer. The variation of the buffer pH had an influence on the pH_M especially within tablet layers without IBS. An additional lipophilic inter layer strongly improved the integrity of both layers. Furthermore, it acted as pH neutral region which could decrease diffusion processes between the layers and therefore influence the pH gradient processing. BT-MRI was accomplished to gain a deeper insight on the differences of proceeding processes during hydration of 2- and 3-layer tablets. The protective character of the inter layer was confirmed which could prevent water penetration between the HPMC and the KSR layer, leading to the aforementioned advantages. Mechanical stress influenced the hydration process as well, which was monitored using different hydration settings. Moreover, an influence of the pH_M on the drug release of the weakly acidic drug Ketoprofen could be demonstrated. In contrast, the drug release of Metformin-HCl, showing pH independent solubility, was not influenced by varied pH_M, as expected.

Acknowledgements

The authors would like to thank Dr. Hendrik Metz for his support concerning EPR and MRI measurements and valuable scientific discussions.

References

Adhikary, A., Vavia, P.R., 2008. Bioadhesive ranitidine hydrochloride for gastroretention with controlled microenvironmental pH. Drug Dev. Ind. Pharm. 34, 860–869.
Akiyama, Y., Yoshioka, M., Horibe, H., Hirai, S., Kitamori, N., Toguchi, H., 1994. pH-independent controlled-release microspheres using polyglycerol ester-fatty acids. J. Pharm. Sci. 83, 1600–1607.
Badawy, S.I., Hussain, M.A., 2007. Microenvironmental pH modulation in solid dosage forms. J. Pharm. Sci. 96, 948–959.
BASF AG, 1999. Technical Information for Kollidon SR. Ludwigshafen, Germany.
Brunner, A., Mäder, K., Göpferich, A., 1999. The microenvironment inside biodegradable microspheres: changes in pH and osmotic pressure. Pharm. Res. 16, 852–858.
Ching, A.L., Liew, C.V., Chan, L.W., Heng, P.V.S., 2008. Modifying matrix microenvironmental pH to achieve sustained drug release from highly laminating alginate matrices. Eur. J. Pharm. Sci. 33, 361–370.
Cope, S.J., Hibberd, S., Whetstone, J., MacRae, R.J., Melia, C.D., 2002. Measurement and mapping of pH in hydrating pharmaceutical pellets using confocal laser scanning microscopy. Pharm. Res. 19, 1554–1563.
Costa, P., Lobo, J.M.S., 2001. Influence of dissolution medium agitation on release profiles of sustained-release tablets. Drug Dev. Ind. Pharm. 27, 811–817.
Doherty, C., York, P., 1989. Microenvironmental pH control of drug dissolution. Int. J. Pharm. 50, 223–232.
Gibaldi, M., 1984. Biopharmaceutics and Clinical Pharmacokinetics. Lea and Febiger, Philadelphia.
Glombitza, B.W., Schmidt, P.C., 1995. Surface acidity of solid pharmaceutical excipients. Part 2. Effect of the surface acidity on the decomposition rate of acetylsalicylic acid. Eur. J. Pharm. Biopharm. 41, 114–119.
Glombitza, B.W., Oelkrug, D., Schmidt, P.C., 1994. Surface acidity of solid pharmaceutical excipients. Part 1. Determination of the surface acidity. Eur. J. Pharm. Biopharm. 40, 289–293.
Grundy, J.S., Foster, R.T., 1996. The nifedipine gastrointestinal therapeutic system (GITS). Evaluation of pharmaceutical, pharmacokinetic and pharmacological properties. Clin. Pharmacokinet. 30, 28–51.
Gutsche, S., Krause, M., Kranz, H., 2008. Strategies to overcome pH-dependent solubility of weakly basic drugs by using different types of alginates. Drug Dev. Ind. Pharm. 34, 1277–1284.
Ingani, H.M., Timmermans, J., Möes, A.J., 1987. Conception and in vivo investigation of peroral sustained release floating dosage forms with enhanced gastrointestinal transit. Int. J. Pharm. 35, 157–164.
Jantratid, E., Janssen, N., Reppas, C., Dressman, J.B., 2008. Dissolution media simulating conditions in the proximal human gastrointestinal tract: an update. Pharm. Res. 25, 1663–1676.
Kavanagh, N., Corrigan, O.I., 2004. Swelling and erosion properties of hydroxypropylmethylcellulose (hypromellose) matrices-influence of agitation rate and dissolution medium composition. Int. J. Pharm. 279, 141–152.
Kempe, S., Metz, H., Mäder, K., 2010. Application of Electron Paramagnetic Resonance (EPR) spectroscopy and imaging in drug delivery research – chances and challenges. Eur. J. Pharm. Biopharm. 74, 55–66.
Khramtsov, V.V., Marsh, D., Weiner, L., Grigoriev, I.A., Volodarsky, L.B., 1982. Proton exchange in stable nitroxyl radicals. EPR study of the pH of aqueous solutions. Chem. Phys. Lett. 91, 69–72.
Li, L., Schwendeman, S.P., 2005. Mapping neutral microclimate pH in PLGA microspheres. J. Control. Release 101, 163–173.
Lurie, D., Mäder, K., 2005. Monitoring drug delivery processes by EPR and related techniques – principles and applications. Adv. Drug Deliv. Rev. 57, 1171–1190.
Mäder, K., Bacic, G., Domb, A., Elmalak, O., Langer, R., Swartz, H.M., 1997. Non invasive in vivo monitoring of drug release and polymer erosion from biodegradable polymers by EPR spectroscopy and NMR imaging. J. Pharm. Sci. 86, 126–134.
Malaterre, V., Metz, H., Ogorka, J., Gurny, R., Loggia, N., Mäder, K., 2009. Benchtop-magnetic resonance imaging (BT-MRI) characterization of push–pull osmotic controlled release systems. J. Control. Release 133, 31–36.
Metz, H., Mäder, K., 2008. Benchtop-NMR and MRI – a new analytical tool in drug delivery research. Int. J. Pharm. 364, 170–175.
Metz, H., Bar-Shalom, D., Mäder, K., 2007. Detailed monitoring of the release mechanism from Egalet tablets by ESR and NMR imaging. In: 33rd CRS Annual Meeting, poster.
Nott, K., 2010. Magnetic resonance imaging of tablet dissolution. Eur. J. Pharm. Biopharm. 74, 78–83.
Pudipeddi, M., Zannou, E.A., Vasanthavada, M., Dontabhaktuni, A., Royce, A.E., Joshi, Y.M., Serajuddin, A.T.M., 2008. Measurement of surface pH of pharmaceutical solids: a critical evaluation of indicator dye-sorption method and its comparison with slurry pH method. J. Pharm. Sci. 97, 1831–1842.
Rahman, Z., Ali, M., Khar, R.K., 2006. Design and evaluation of bilayer floating tablets of captopril. Acta Pharm. 56, 49–57.
Richardson, J.C., Bowtell, R.W., Mäder, K., Melia, C.D., 2005. Pharmaceutical applications of magnetic resonance imaging (MRI). Adv. Drug Deliv. Rev. 57, 1191–1209.
Riis, T., Bauer-Brandl, A., Wagner, T., Kranz, H., 2007. pH-independent drug release of an extremely poorly soluble weakly acidic drug from multiparticulate extended release formulations. Eur. J. Pharm. Biopharm. 65, 78–84.
Schädlich, A., Ullrich, S., Mäder, K., 2009. In vivo pH measurements of in situ forming sucrose ester implants using multispectral fluorescence imaging. In: Poster, 36th Annual Meeting and Exposition of the Controlled Release Society, Copenhagen.
Scheef, C.A., Oelkrug, D., Schmidt, P.C., 1998. Surface acidity of solid pharmaceutical excipients. III. Excipients for solid dosage forms. Eur. J. Pharm. Biopharm. 46, 209–213.
Sheng, J.J., Kasim, N.A., Chandrasekharan, R., Amidon, G.L., 2006. Solubilization and dissolution of insoluble weak acid, ketoprofen: effects of pH combined with surfactant. Eur. J. Pharm. Sci. 29, 306–314.
Siepe, S., Lueckel, B., Kramer, A., Ries, A., Gurny, R., 2006. Strategies for the design of hydrophilic matrix tablets with controlled microenvironmental pH. Int. J. Pharm. 316, 14–20.
Streubel, A., Siepmann, J., Dashevsky, A., Bodmeier, R., 2000. pH-independent release of a weakly basic drug from water-insoluble and -soluble matrix tablets. J. Control. Release 67, 101–110.
Strübing, S., Abboud, T., Contri, R.V., Metz, H., Mäder, K., 2008a. New insights on Polyvinylacetate based coated floating tablets: characterisation of hydration and CO_2 generation by benchtop MRI and its relation to drug release and floating strength. Eur. J. Pharm. Biopharm. 69, 708–717.
Strübing, S., Metz, H., Mäder, K., 2008b. Characterization of polyvinyl acetate based floating matrix tablets. J. Control. Release 126, 149–155.
Tatavarti, A.S., Hoag, S.W., 2006. Microenvironmental pH modulation based release enhancement of a weakly basic drug from hydrophilic matrices. J. Pharm. Sci. 95, 1459–1468.

Tatavarti, A.S., Mehta, K.A., Augsburger, L.L., Hoag, S.W., 2004. Influence of methacrylic and acrylic acid polymers on the release performance of weakly basic drugs from sustained release hydrophilic matrices. J. Pharm. Sci. 93, 2319–2331.

Thoma, K., Zimmer, T., 1990. Retardation of weakly basic drugs with diffusion tablets. Int. J. Pharm. 58, 197–202.

Tran, P.H.L., Tran, H.T.T., Lee, B.-J., 2008. Modulation of microenvironmental pH and crystallinity of ionizable telmisartan using alkalizers in solid dispersions for controlled release. J. Control. Release 129, 59–65.

Varma, M.V.S., Kaushal, A.M., Garg, S., 2005. Influence of micro-environmental pH on the gel layer behavior and release of a basic drug from various hydrophilic matrices. J. Control. Release 103, 499–510.

Wei, Z., Yu, Z., Bi, D., 2001. Design and evaluation of a two-layer floating tablet for gastric retention using cisapride as a model drug. Drug Dev. Ind. Pharm. 27, 469–474.

Zinchuck, A.V., Hancock, B.C., Shalaev, E.Y., Reddy, R.D., Govindarajan, R., Novak, E., 2005. The influence of measurement conditions on the Hammett acidity function of solid pharmaceutical excipients. Eur. J. Pharm. Biopharm. 61, 158–170.